Published in final edited form as:
J Bone Miner Res. 2011 September ; 26(9): 2012–2025. doi:10.1002/jbmr.417.

Genetic Evidence Points to an Osteocalcin-independent Influence of Osteoblasts on Energy Metabolism

Yoshihiro Yoshikawa[1,5], **Aruna Kode**[1], **Lili Xu**[1,6], **Ioanna Mosialou**[1], **Barbara C. Silva**[1], **Mathieu Ferron**[2], **Thomas L. Clemens**[3], **Aris N. Economides**[4], and **Stavroula Kousteni**[1,*]

[1]Department of Medicine, Division of Endocrinology, College of Physicians & Surgeons, Columbia University, New York, NY, USA

[2]Department of Genetics and Development, College of Physicians & Surgeons, Columbia University, New York, NY, USA

[3]Center for Musculoskeletal Research, Department of Orthopedic Surgery, Johns Hopkins University, Baltimore, MD USA

[4]Bone & Cartilage Biology Group, Genome Engineering Technologies Group Regeneron Pharmaceuticals, Inc, Tarrytown, NY, USA

Abstract

The skeleton has recently been shown to regulate glucose metabolism through an osteoblast-specific hormone, osteocalcin, which favors β-cell proliferation, insulin secretion, insulin sensitivity and energy expenditure. An implication of this finding is that a decrease in osteoblast numbers would compromise glucose metabolism in an osteocalcin-dependent manner. To test this hypothesis osteoblasts were inducibly ablated by cross-breeding transgenic mice expressing a tamoxifen-regulated Cre under the control of the osteocalcin promoter with mice in which an inactive form of the diphtheria toxin A chain is introduced into a ubiquitously expressed locus. Ablation of osteoblasts in adult mice profoundly affected glucose metabolism. In a manner similar to what is seen in the case of osteocalcin deficiency, a partial ablation of this cell population resulted in hypoinsulinemia, hyperglycemia, glucose intolerance and decreased insulin sensitivity. However, and unlike what is seen in osteocalcin-deficient mice, osteoblast ablation also decreased gonadal fat, increased energy expenditure and the expression of resistin, an adipokine proposed to mediate insulin resistance. While, administration of osteocalcin reversed, fully, the glucose intolerance and reinstated normal blood glucose and insulin levels, it only partially restored insulin sensitivity and did not affect the improved gonadal fat weight and energy expenditure in osteoblast-depleted mice. These observations not only strengthen the notion that osteoblasts are necessary for glucose homeostasis and energy expenditure, but they also suggest that in addition to osteocalcin, other osteoblast-derived hormones may contribute to the emerging function of the skeleton as a regulator of energy metabolism.

Keywords

Osteoblasts; osteocalcin; glucose; energy metabolism

[*]To whom correspondence should be addressed. Mailing address: The Russ Berrie Medical Sciences Pavilion 1150 Saint Nicholas Avenue Room 312 New York, NY, 10032 TEL: 212-851-5223 FAX: 212-851-5225 sk2836@columbia.edu.
[5]Current address: Department of Biochemistry, Osaka Dental University, Osaka, Japan
[6]Current address: Mount Sinai Medical Center, New York, NY, USA

The authors do not have any conflicts of interest.

Introduction

In the last few years, skeletal physiology has expanded to cover areas that are beyond longitudinal growth, bone mass homeostasis and bone mineralization or the mechanisms by which diseases affect bone mass. Notably, the skeleton has emerged as an important regulator of energy metabolism (1-3). Osteocalcin, a secreted protein that is specifically expressed by osteoblasts, is essential in mediating this novel endocrine function of the skeleton. Osteocalcin acts as a hormone to increase β-cell proliferation, insulin secretion and sensitivity and energy expenditure. The combined hyperinsulinemia and improved insulin sensitivity result in improved glucose tolerance and glucose metabolism. In a leap forward from the studies in rodents, many clinical studies have suggested that osteocalcin is a marker of glucose tolerance (1;3-7). Furthermore, two transcription factors, one osteoblast-enriched, ATF4, and one more broadly expressed, FoxO1, inhibit insulin secretion and sensitivity in its peripheral target organs through their expression in osteoblasts (8;9). They achieve this task by suppressing osteocalcin activity. Thus, multiple genes, some ubiquitously expressed others osteoblast-enriched if not specific, conquer to affect glucose metabolism through their expression in osteoblasts.

The existence of one bone-derived hormone regulating energy metabolism raises the question of whether other hormonal signals originating from the osteoblasts influence the ability of the skeleton to maintain energy homeostasis. A global ablation of osteoblasts could be a useful tool as a first attempt to address these important questions of bone physiology. Indeed, cell ablation has proven in many instances to be a powerful way for delineating the function of particular cell types in various organs including the skeleton (10-15).

We report here the generation of a mouse model of inducible osteoblast ablation. Analysis of this model verified, as expected, the role of osteoblasts in glucose homeostasis. Remarkably, however, our results indicate that osteoblasts have the ability to affect glucose metabolism through both osteocalcin-dependent and independent mechanisms. Hence, this work suggests that other molecules secreted by osteoblasts and, yet to be identified, affect energy metabolism.

Materials and Methods

Mice

The *ROSA26-lacZ*$^{fl/fl}$ mice were obtained from Jackson Laboratories (*GtROSA26*^{tm1Sho}) (16). The DTA mice were generated as follows. A Cre-regulated diphtheria toxin A chain (*DTA*) mini-gene was engineered into the *Gt(ROSA)26Sor* locus by targeting a 'floxed STOP' cassette (*3′SS-LoxP-EM7-neo-pgkpolyA-tpA-LoxP*) followed by an cDNA encoding for dta-ires-eGFP-ßglpA into the *XbaI* site of the *Gt(ROSA)26Sor* locus (coordinates 113026025 to 113026030 on Chromosome 6, Ensembl release 60 - Nov 2010). 3′ SS is a 3′ splice region consensus region (CTA GTT CCC TTT TTT TTC ACA G), EM7 is a prokaryotic promoter, neo is a neomycin phophotransferase ORF (17), pgkpA is a polyadenylation region derived from the phosphoglycerate kinase gene (18), tpA is a polyadenylation region comprised of 3 tandem copies of an SV40-derived polyadenylation region (16), *DTA* is an ORF encoding for diphtheria toxin A (19), IRES is an internal ribosome entry site, eGFP is an enhanced Green Fluorescent Protein, and ßglpA is a polyadenylation region derived from the rabbit beta globin gene. The floxed STOP cassette is identical to that utilized previously (Soriano, 1999), except that neo is lacking a mammalian promoter. This engineering modality renders its expression is dependent on integration into a transcriptionally active locus, and can thereby 'facilitate' targeting by reducing the number of non-productive integrations. Targeting is guided to the

Gt(ROSA)26Sor locus by flanking this cassette and *DTA-ires-eGFP-ßglpA* module with homology arms comprised of ~2.4 and ~2.8 kb 5′ and 3′ of the XbaI site. Targeting was performed into CJ7 ES cells as described (20); 6 out of 40 colonies screened were correctly targeted. Of these, VG2128A-H4 and VG2182B-G5 were microinjected to generate mice. Mice harboring this targeted integration (*Gt(ROSA)26Sor*$^{floxed\text{-}STOP\_dta/+}$) are termed DTAfl/fl and were physiologically normal, indicating that no DTA protein was expressed prior to removal of the floxed STOP region. The *OCN-Cre-ER*^{T2} transgene was constructed by fusing the human osteocalcin promoter and a cDNA encoding *Cre-ER*^{T2}. The plasmid *pKB-Cre-ER*^{T2} (21) was cleaved with NotI and KpnI to isolate the *Cre-ER*^{T2} cDNA. The *Cre-ER*^{T2} fragment was then subcloned into pOC, which contains 3,900 bp of the human osteocalcin promoter and the second intron of rabbit β-globin on a pBluescript SK(−) backbone (22), to create *pOC-Cre-ER*^{T2}. The insert of this plasmid (*OC-Cre-ER*^{T2}) was excised and microinjected into fertilized eggs (FVB-N mouse strain). The wild-type and *DTA*^{flox} alleles were detected using PCR with primers 5′-TGTGGACAGAGGAGCCATAA-3′ and 5′-TGGCTCATTAGGGAATGCTT-3′ (for wild-type) and 5′-TGTGGACAGAGGAGCCATAA-3′ and 5′-CTCGTCCTGCAGTTCATTCA-3′ (for the *DTA*^{flox} allele). Genotyping was performed at 3 weeks of age by PCR analysis of genomic DNA. In all experiments data presented were obtained from male animals. All procedures were approved by the Institutional Animal Care and Use Committee.

β-galactosidase staining

Femurs from 2-month-old *ROSA26-lacZ*$^{fl/fl}$ and *OCN-CreER*^{T2} double mutant mice (*i-LacZ*$_{osb}$) as well as from *ROSA26-lacZ*$^{fl/fl}$ controls mice were fixed in 10% formalin and stained whole mount in X-gal staining solution for 16 hours. After staining, femurs were decalcified, embedded in paraffin and sectioned at a thickness of 7μm.

Recombinant Uncarboxylated Osteocalcin Purification

Purification of bacterially produced mouse recombinant uncarboxylated osteocalcin was performed as described previously (1;2). Briefly, the sequence encoding for mature osteocalcin was cloned in pGEX2TK vector and GST-osteocalcin fusion protein was bacterially produced and purified on glutathione-Sepharose according to standard procedures. After extensive washes, osteocalcin was then cleaved out from the GST moiety by using thrombin. A HiTrap Benzamidine column was subsequently used to deplete the thrombin from the preparation. Purity (>95%) of the osteocalcin preparation was assessed by Tris-Tricine SDS/PAGE stained with Coomassie Blue. Concentration and integrity of the recombinant osteocalcin protein was precisely determined by using osteocalcin RIA (Immunotopic).

Histological analysis of pancreatic islets, white adipose tissue and liver sections—Histological analysis was performed as previously described (9). Briefly, fat and pancreata were collected, fixed overnight in 10% neutral formalin solution, embedded in paraffin, sectioned at 4 μm and stained with hematoxylin and eosin (H&E). Pancreatic sections were immunostained for β cells using guinea pig anti-swine insulin polyclonal antibody (Dako). β-cell proliferation was assessed using an antibody recognizing Ki67 antigen, the prototypic cell cycle related nuclear protein expressed by proliferating cells in all phases of the active cell cycle. β-cell area represents the surface positive for insulin immunostaining divided by the total pancreatic surface. β-cell mass was calculated as β-cell area multiplied by pancreatic weight. Livers were cryoembedded, sectioned at 5μm and stained with Oil red O (Crystalgen).

Cell cultures—Primary osteoblasts were prepared from calvaria of 5 day-old pups as previously described (1) and were cultured in fresh αMEM and 10% FBS.

Real-time quantitative PCR analysis—DNAse I (Invitrogen) treated RNA was reverse transcribed at 42°C with SuperScript II (Invitrogen). The expression of all the genes was measured by real-time quantitative PCR with the syber green master mix using 18S as endogenous control with 1 cycle at 95°C for 10 minutes followed by 40 cycles at 95°C for 30 seconds and 60°C for 1 minute.

Metabolic studies—Intraperitoneal glucose tolerance test was performed by administering 2 g of glucose per kg of body weight (BW) intraperitoneally (IP) after an overnight fast. Blood glucose was monitored using blood glucose strips (Diabetes association) and the Accu-Check glucometer. For insulin tolerance test (ITT) mice were fasted from 4- 6 hours, injected IP with insulin (0.5U/kg BW) and blood glucose levels were measured at indicated times. ITT data are presented as percentage of initial blood glucose concentration.

Physiological assays—Sera were collected by heart puncture from mice in the fed state. Blood was kept on ice for 15 min before centrifugation for 15 min, at maximum speed. Insulin (Mercodia), Adiponectin (Millipore), leptin (Crystal Chem) levels were measured by ELISA.

Energy balance—Energy expenditure was measured by indirect calorimetric method using a six-chamber Oxymax system (Columbus Instruments, Ohio) as described (9). Food consumption was determined by weighing the powdered chow before and after the 24-hour measurement.

Statistical analyses—Results are given as means ± SEM. Statistical analyses relied on independent two-tailed Student's *t* for between group comparisons or one-way ANOVA with Tukey HSD range test for pair-wise comparisons when 3 or more groups are involved. Critical test statistics with p-values less than 0.05 are considered statistically significant.

Results

Generation and characterization of mice for inducible inactivation of osteoblasts

Inducible ablation of osteoblasts was achieved by cross-breeding transgenic mice expressing a tamoxifen-regulated Cre under the control of the human osteocalcin promoter (*OCN-CreER*^{T2}) with mice in which an inactive form of the diphtheria toxin A chain (*DTA*) has been introduced into the ubiquitously expressed ROSA26 locus (*DTA*$^{fl/fl}$, Figure 1A). The OCN promoter has been successfully used to direct strong osteoblast-specific expression of various genes in transgenic mice [22-26]. In the *DTA* mice, *DTA* expression is prevented by the presence of a DNA STOP sequence which terminates transcription flanked by two loxP sites. *DTA*$^{fl/fl}$ mice were healthy and fertile. *ER*^{T2} is a second generation mutant of the hormone-binding domain of the human estrogen receptor (ER) which gives a 4-fold increase in the efficiency of recombination induced by 4-hydroxy-tamoxifen and reduces problems with slow response in gene expression following the cessation of treatment (21). We relied on this approach because it has been successfully used to induce cell-specific killing in a variety of murine models (27-29).

As a first means to ascertain the functionality of tamoxifen-induced Cre activity in the *OCN-CreER*^{T2} mouse model, we crossed *OCN-CreER*^{T2} mice with *ROSA26-lacZ*$^{fl/fl}$ mice (16). The *ROSA26-lacZ*$^{fl/fl}$ reporter mouse line consists of the *lacZ* gene preceded by a

transcriptional stop cassette that is flanked by two *loxP* sites. Upon tamoxifen treatment, the Cre recombinase should be activated, and the stop cassette removed, thereby inducing the expression of β-galactosidase (β-gal) in all cell populations of interest. Adult, compound mutant mice carrying both the *ROSA26-lacZ*$^{fl/fl}$ allele and the *OCN-CreER*^{T2} transgene (*i-LacZ*$_{osb}$, for inducible expression of *LacZ* in osteoblasts) were treated with tamoxifen for 10 days. Expression of β-gal was detected in the nucleus of osteoblasts, seen as cuboid cells on the surface of bone, and in osteocytes in the femoral primary spongiosa and also in the femoral midshaft from *i-LacZ*$_{osb}$ mice treated with tamoxifen but not vehicle (Figures 1B-E). Thus, these results indicate that Cre is efficiently and specifically expressed in osteoblasts and osteocytes following administration of tamoxifen to live animals. Lastly, the dose of tamoxifen used had no detectable toxic effects.

Progeny of crosses between *DTA*$^{fl/fl}$ mice and *OCN-CreER*^{T2} mice were functionally characterized for DTA activity. For this purpose, compound mutant mice were treated either with vehicle (*DTA* mice) or with tamoxifen (*DTA*$_{osb}$, for inducible expression of *DTA* in osteoblasts). Treatment of primary osteoblasts derived from the *DTA*$_{osb}$ double mutant mice, but not from *DTA*$^{fl/fl}$ control animals, with tamoxifen resulted in 55% apoptosis Figure 1F). These data indicate that the *DTA* locus can be successfully activated by the *OCN-CreER*^{T2} transgene upon exposure to tamoxifen, to efficiently, although partially, ablate osteoblasts.

Low bone mass and bone formation with inducible, partial osteoblast ablation in DTA$_{osb}$ mice

Adult *DTA* mice and wild type littermates (*DTA*$^{fl/fl}$, termed WT) were injected intraperitoneally (i.p) with vehicle or 0.07mg/g of tamoxifen daily for 10 days and the effect of inducible *DTA* expression on bone was examined. Tamoxifen-treated *DTA*$_{osb}$ mice were characterized by a 50% reduction in osteoblast numbers (N.Ob./T.Ar.), bone formation rate (BFR) and bone volume (BV/TV) as compared to vehicle-treated *DTA* mice or wild type animals (Figures 1G-I). Bone resorption increased as indicated by the increase in osteoclast surface in *DTA*$_{osb}$ as compared to WT control mice (Figure 1J) These data verified the efficiency of osteoblast ablation in bone and its effect on bone homeostasis.

Increased blood glucose levels, glucose intolerance and insulin insensitivity in mice lacking osteoblasts

To determine the consequences, if any, of the reduction of osteoblast numbers in *DTA*$_{osb}$ mice on glucose metabolism, we examined the metabolic phenotype of these animals. Measurements of blood glucose levels revealed a 1.8-fold increase in blood glucose levels in *DTA*$_{osb}$ mice as compared to *DTA* or WT animals (Figure 2A). The observed hyperglycemia was due to, at least in part, a 2-fold decrease in insulin levels (Figure 2B). The decrease in insulin synthesis was due to a reduction in β-cell area and mass and in islet numbers (Figures 2C-E), and β-cell proliferation (Figure 2F). As expected given this decrease in insulin secretion, disposal of a glucose load, tested by glucose tolerance tests (GTT), was compromised by osteoblast ablation in *DTA*$_{osb}$ mice as indicated by a decrease in glucose tolerance as compared to *DTA* or WT animals (Figure 2G). Total fat content (Figure 2H) and body weight (Figure 2I) were not affected in *DTA*$_{osb}$ mice, whereas lean body mass was decreased by osteoblast ablation in these mice (Figure 2J). Since, osteocalcin deficiency causes the same metabolic abnormalities in glucose handling we examined whether osteocalcin levels were altered in the osteoblast-deficient *DTA*$_{osb}$ mice. Measurements of osteocalcin expression and serum levels indicated a 50% reduction in *DTA*$_{osb}$ mice as compared to *DTA* or WT control mice (Figures 3A-B). These results establish that even a partial reduction in osteoblasts numbers is sufficient to induce hyperglycemia and glucose intolerance and reduce lean mass, at least in part through

inhibition of insulin production. As such, they are consistent with the role of osteocalcin in glucose metabolism.

Recombinant Osteocalcin normalizes glucose levels and tolerance in DTA_{osb} osteoblast-depleted mice

As a first way to determine whether the glucose intolerance phenotype of the osteoblast-depleted DTA_{osb} mice was caused, solely, by a decrease in osteocalcin secretion we examined whether administration of recombinant uncarboxylated osteocalcin would rescue the metabolic phenotype resulting from partial osteoblast ablation in these animals. For this purpose, adult DTA_{osb} mice and WT littermates were injected i.p. with vehicle or 0.07mg/g of tamoxifen daily for 10 days. At this time, mice were either left untreated or were treated i.p. with 30 ng/g per day of recombinant osteocalcin for 4 weeks. This dose of osteocalcin has been shown previously to improve glucose metabolism in WT mice (30). At the end of the 4 weeks period we verified that osteocalcin levels were restored in DTA_{osb} mice. Exogenous osteocalcin restored normal levels of osteocalcin in DTA_{osb} mice (Figure 3C). As expected, the increase in osteocalcin levels suppressed the increased glucose production in DTA_{osb} mice to WT levels and restored normal glucose tolerance (Figures 3D-E). The improvement of glucose metabolism following osteocalcin administration was associated with reestablishment of normal levels of serum insulin (Figure 3F) as well as pancreatic function in DTA_{osb} mice (Figures 3G-J). Indeed, the decreased β-cell area, β-cell mass and islet numbers as well as the decrease in β-cell proliferation in DTA_{osb} mice were all rescued by osteocalcin administration. Hence, the imbalance in glucose metabolism caused by osteoblast ablation appears to be due to a decrease in osteocalcin synthesis and secretion.

Differential effects of osteoblast ablation and osteocalcin in insulin sensitivity, gonadal fat weight and energy expenditure

To determine whether osteocalcin is the only osteoblast-derived molecule regulating energy metabolism we examined potential changes caused by osteoblast ablation in other metabolic parameters determining energy homeostasis. In addition to hypoinsulinemia, changes in insulin sensitivity may contribute to the hyperglycemia and glucose intolerance caused by osteoblast ablation in DTA_{osb} mice. Indeed, insulin tolerance tests (ITT) showed that DTA_{osb} mice were characterized by insulin insensitivity as compared to WT animals (Figure 4A). This phenotype is also in agreement with the insulin insensitivity phenotype of osteocalcin-deficient mice(1), however it was consistently more severe in DTA_{osb} mice than what has been shown in osteocalcin-deficient mice. Therefore we examined whether osteocalcin administration would restore fully insulin sensitivity in DTA_{osb} mice. Recombinant osteocalcin only partially normalized insulin sensitivity in osteoblast-deficient DTA_{osb} mice (Figure 4B). To uncover the mechanism leading to an increase in insulin sensitivity with osteoblast ablation, we studied the expression of three adipokines known to influence insulin resistance; resistin, adiponectin and leptin. In agreement with the observed insulin insensitivity, serum levels of the insulin-sensitizing hormone *adiponectin* (31) were decreased whereas expression of *Resistin*, an adipokine which mediates insulin resistance (32), was increased by partial osteoblast ablation in DTA_{osb} mice (Figures 4C-D). As expected, osteocalcin administration reversed the decrease in adiponectin serum levels in mice lacking osteoblasts and increased adiponectin production in DTA and WT animals (Figure 4E), however, it had no effect on *Resistin* levels, in either WT or osteoblast-depleted DTA_{osb} mice (Figure 4F). Serum levels of the insulin-sensitizing hormone Leptin (33) were not affected by either osteoblast deficiency or osteocalcin administration (Figures 4G). These results suggest that osteoblasts may affect glucose metabolism in an osteocalcin-independent manner.

The differential changes in the regulation of adiponectin and resistin production caused by osteoblast ablation versus osteocalcin deficiency prompted us to examine the effect of osteoblasts on white adipose tissue. Despite their hypoinsulinemia and insulin insensitivity, and in contrast to the phenotype of osteocalcin deficiency, DTA_{osb} mice had decreased gonadal fat weight as compared to *DTA* or WT animals (Figure 5A). Adipocyte numbers were also decreased by osteoblast ablation (Figure 5B). Exogenous osteocalcin did not further suppress gonadal fat weight or adipocyte numbers in DTA_{osb} mice (Figures 5C-D). Respective to the effect in gonadal fat weight, osteoblast ablation reduced expression of the adipogenic gene *C/EBPα* and increased expression of two lipolytic genes *Triglyceride lipase* (*Tgl*) and *Perillipin*, whose expression is inhibited by insulin (Figures 5E-G). In contrast to the lack of an effect with osteocalcin deficiency (1), osteoblasts ablation increased the expression of *lipoprotein lipase* (*Lpl*) (Figure 5H). Again, osteocalcin administration had no effect on the expression of *C/EBPα* but suppressed *Tgl* and *Perillipin* expression in mice with normal (*DTA*) and ablated (DTA_{osb}) osteoblasts as well as *Lpl* expression in DTA_{osb} mice. These results suggest that osteoblast ablation decreases adipogenesis independent of osteocalcin but promotes lipolysis and lipogenesis in an osteocalcin-dependent manner.

To understand the reason for the decrease in gonadal fat weight, despite the hyperglycemia and insulin insensitivity, we examined whether osteoblast ablation affected energy expenditure. Explaining, at least in part, the decrease in gonadal fat weight, energy expenditure was increased in DTA_{osb} mice as compared to *DTA* animals (Figure 6A). Oxygen and CO_2 consumption were also increased by osteoblast ablation (Figures 6B-C). Interestingly, food intake was increased whereas activity was decreased by osteoblast ablation in DTA_{osb} mice (Figures 6D-E). Osteocalcin administration did not further improve the increased energy expenditure in DTA_{osb} mice (Figures 6F-H) and had no effect on food intake (Figure 6I) or movement in either DTA_{osb} or *DTA* animals (Figure 6J). These data indicate that, similar to the decrease in gonadal fat, the increase in energy expenditure in DTA_{osb} mice was opposite to what would be expected if osteocalcin was the sole osteoblast-derived hormone regulating these parameters.

The liver is another source of glucose production and a target of insulin signaling. Thus, we examined whether insulin signaling or functions responsive to insulin in the liver were affected by osteoblast ablation. Liver fat content was decreased in DTA_{osb} mice as compared to *DTA* animals (Figure 7A). In spite of the decrease in fat content, expression of *FoxA2*, which activates transcriptional programs of lipid metabolism and ketogenesis during fasting and is downregulated by insulin signaling (34), was increased by osteoblast ablation in DTA_{osb} mice (Figure 7B). This apparent discrepancy can be explained by the fact that insulin resistance, caused by osteoblast ablation, inactivates *FoxA2* by permanently locating it in the cytoplasm of hepatocytes (34). Remarkably, osteocalcin had no effect on *FoxA2* expression or fat content further indicating that osteoblasts may regulate lipogenesis and ketogenesis in an osteocalcin-independent manner. In the hepatocyte decreased insulin signaling promotes gluconeogenesis by acting in concert with the PPARγ coactivator PGC1α to stimulate the expression of glucose-6-phosphatase (*G6pase*) and phosphoenolpyruvate kinase 1 (*Pepck1*) (35). Consistent with the hypoinsulinemia and insulin insensitivity, and as seen in osteocalcin-deficiency, expression of *Pepck1* increased in DTA_{osb} mice suggesting that osteoblast ablation promotes gluconeogenesis (Figure 7C). In contrast to osteocalcin-deficiency expression of *G6pase* was decreased with osteoblast ablation (Figure 7D). As expected, osteocalcin treatment decreased the expression of both genes in WT mice.

Finally, due to the recently discovered role of osteocalcin in promoting male fertility (36), we examined whether osteoblast ablation would affect this particular endocrine function of the skeleton. As expected, osteocalcin administration increased serum testosterone in DTA

mice (Figure 7E). Similar to osteocalcin deficiency, osteoblast ablation suppressed testosterone levels; and, exogenous osteocalcin in mice lacking osteoblasts reversed this suppression and restosted testosterone to normal serum levels.

Discussion

The results presented in this study, prove that the skeleton, acts through the osteoblasts to potently regulate all determinants of energy metabolism: glucose and insulin production, glucose tolerance and insulin sensitivity, fat metabolism, energy expenditure and appetite in both osteocalcin-dependent and independent manners (Figure 7F). Indeed, a partial, only 50% reduction in osteoblast numbers was sufficient to dramatically compromise glucose homeostasis and metabolism of all insulin target tissues examined, pancreas, liver and white adipose tissue.

A comparison between multiple metabolic parameters showed that some metabolic changes induced by osteoblast ablation were a) rescued by osteocalcin treatment, and b) in the same direction as those induced by osteocalcin deficiency (for a direct comparison see Table 1). Other abnormalities, such as gonadal fat weight, energy expenditure, food intake and hepatic responses could not be explained by a lack of osteocalcin since osteocalcin-deficient mice do not harbor them. In reviewing these changes it appears that whereas osteocalcin is the hormone that regulates glucose tolerance, β-cell proliferation and insulin secretion, additional bone-derived proteins may be affecting insulin sensitivity, gonadal fat weight, hepatic glucose production and energy expenditure and intake. These data indicate that, similar to the decrease in gonadal fat, the increase in energy expenditure in DTA_{osb} mice was opposite to what would be expected if osteocalcin was the sole osteoblast-derived hormone regulating these parameters. Indeed, osteocalcin deficiency decreases energy expenditure and increases gonadal fat weight (1). Likewise, whereas appetite is increased by osteoblast ablation, it is not affected by osteocalcin deficiency (1) or treatment (Figure 6I), further supporting the notion of a more complex regulation of energy expenditure and appetite by osteoblasts that involves both osteocalcin-dependent and independent responses. The observation that appetite is affected by osteoblast ablation advances our knowledge of the role of the skeleton as a regulator of energy metabolism a step further. It suggests that, osteoblasts may secrete hormone(s) capable of directly or indirectly affecting food intake.

In our mouse model osteoblast ablation resulted in a parallel decrease in gonadal fat weight as well as adipocyte numbers, suggesting a linear correlation between these two cell types. Interestingly, it is thought that osteoblasts and adipocytes originate from a common marrow mesenchymal stem cell (MSC) in the bone marrow niche (37); and, that differentiation of MSCs into one of two lineages during the process of adipogenesis and osteoblastogenesis are mutually exclusive. Lending support to this hypothesis, adipocytes gradually infiltrate long bones marrow during pubertal growth; and adipocyte numbers increase in the bone marrow (fatty marrow) with advancing age. Importantly, these age-related changes in marrow adiposity are associated with bone loss. These observations are recapitulated in older mice, where expression of PPARγ, a master regulator of adipocyte differentiation, lipid biosynthesis and insulin sensitivity are highly increased in marrow-derived MSCs (38). Genetic or pharmacological inactivation of PPARγ, represses adipogenesis but stimulates osteoblastogenesis (39;40). Similarly, in mice heterozygous for *Pparγ* bone mass is high, and osteoblast differentiation markers are enhanced (41). Additionally, adipocyte-specific deletion of *Pparγ* in mice results in lipodystrophy in parallel to high bone mass. However, some lines of evidence contradict mutual exclusivity for lineage allocation. For example, activation of PPARγ with a partial agonist does not cause trabecular bone loss despite a substantial increase in the number of marrow adipocytes (42). Similarly, C3H/HeJ, an inbred mouse strain, has very high bone mass but more marrow adiposity than C57BL/6J

throughout development. Finally, mice lacking the transcription factor *Ebf1* are lipodystrophic but have high bone mass and a large increase in bone marrow adipocytes with enhanced PPARγ expression (43). We believe that our experimental model does not exclude a linear specification scheme that diverges early between fat and bone. Instead, it may suggest that osteoblasts secrete more than one proteins that differentially affect adipocyte fate. If that were the case, the purpose of such an opposing type of regulation would be to maintain homeostasis. Alternatively, an earlier cell at the osteoblast lineage rather than the osteocalcin-expressing osteoblast, which we have ablated, may be the cell that is inversely related to the adipocyte.

A novel, recently reported property has been added in the function of the skeleton as an endocrine organ. Again through the actions of osteocalcin, the skeleton regulates male fertility by promoting testosterone synthesis (36). Similar to the case of osteocalcin deficiency we found that osteoblast ablation reduces testosterone levels in male mice and osteocalcin administration reverses this decreases and restores testosterone to normal levels. These results indicate that the ability of the skeleton to regulate male fertility is osteocalcin-dependent.

Taken together, the results of this study expand our understanding of the endocrine function of the skeleton beyond the level of osteocalcin as its sole mediator. They suggest that in addition to osteocalcin, bone produces other hormones which also affect energy metabolism. The notion of an additional, bone-derived hormone regulating glucose metabolism is in line with the fact that other organs utilize more than one secreted molecules to affect body functions. The pituitary, often called the “master gland”, secretes at least 6 specific hormones that affect almost every organ in the body (Thyroid Stimulating Hormone) and regulate a diverse array of body functions from growth (Growth Hormone), maturation and metabolism to stress response (Adrenocorticotropic Hormone), reproduction (Luteinizing and Follicle Stimulating Hormones LH and FSH), breast milk secretion (Prolactin) and water retention (Vasopressin). The ovaries through the production of estrogens and progesterone regulate reproduction, skeletal health, cardiovascular and neurological functions. Inhibin and activin, also produced by the ovaries, regulate biosynthesis and secretion of FSH. Similar to these examples it is reasonable to expect that if the skeleton has the ability to influence glucose metabolism, insulin secretion and sensitivity, energy expenditure and appetite, it must achieve these multiple functions by acting on more that one energy-regulating organs. Indeed previous and the current study indicate that osteoblasts affect insulin signaling and glucose-regulating functions of pancreas, liver, white adipose tissue, muscle. This multifactorial process is also reasonable to be mediated by the actions of more than one osteoblast-derived hormones. These proteins may act either in synergy with osteocalcin, or by counteracting osteocalcin in its metabolic functions. The overall outcome and the purpose of these interactions is glucose homeostasis.

Acknowledgments

The authors are grateful to Dr Gerard Karsenty for helpful discussions and critical reading of the manuscript. We are also thankful to Jayesh G. Shah and Charles Duncan for technical assistance. We are thankful to the histology and metabolic units facilities of the Diabetes and Endocrinology Research Center (DERC) of Columbia University Medical Center (supported by NIDDK DK063608-07) for help with histological analysis. This work was supported by the National Institutes of Health (R01-AR055931, 3-R01-AR055931-02S1 and P01-AG032959).

Reference List

1. Lee NK, Sowa H, Hinoi E, Ferron M, Ahn JD, Confavreux C, Dacquin R, Mee PJ, McKee MD, Jung DY, Zhang Z, Kim JK, Mauvais-Jarvis F, Ducy P, Karsenty G. Endocrine regulation of energy metabolism by the skeleton. Cell. Aug 10.2007 130:456–469. [PubMed: 17693256]

2. Ferron M, Wei J, Yoshizawa T, Del FA, DePinho RA, Teti A, Ducy P, Karsenty G. Insulin Signaling in Osteoblasts Integrates Bone Remodeling and Energy Metabolism. Cell. Jul 23.2010 142:296–308. [PubMed: 20655470]

3. Fulzele K, Riddle RC, Digirolamo DJ, Cao X, Wan C, Chen D, Faugere MC, Aja S, Hussain MA, Bruning JC, Clemens TL. Insulin Receptor Signaling in Osteoblasts Regulates Postnatal Bone Acquisition and Body Composition. Cell. Jul 23.2010 142:309–319. [PubMed: 20655471]

4. Pittas AG, Harris SS, Eliades M, Stark P, wson-Hughes B. Association between serum osteocalcin and markers of metabolic phenotype. J Clin Endocrinol Metab. Mar.2009 94:827–832. [PubMed: 19088165]

5. Kindblom JM, Ohlsson C, Ljunggren O, Karlsson MK, Tivesten A, Smith U, Mellstrom D. Plasma osteocalcin is inversely related to fat mass and plasma glucose in elderly Swedish men. J Bone Miner Res. May.2009 24:785–791. [PubMed: 19063687]

6. Kanazawa I, Yamaguchi T, Yamamoto M, Yamauchi M, Kurioka S, Yano S, Sugimoto T. Serum osteocalcin level is associated with glucose metabolism and atherosclerosis parameters in type 2 diabetes mellitus. J Clin Endocrinol Metab. Jan.2009 94:45–49. [PubMed: 18984661]

7. Saleem U, Mosley TH Jr. Kullo IJ. Serum osteocalcin is associated with measures of insulin resistance, adipokine levels, and the presence of metabolic syndrome. Arterioscler Thromb Vasc Biol. Jul.2010 30:1474–1478. [PubMed: 20395593]

8. Yoshizawa T, Hinoii E, Jung DY, Kajimura D, Ferron M, Seo J, Graff JM, Kim JK, Karsenty G. The transcription factor ATF4 regulates glucose metabolism through its expression in osteoblasts. J Clin Invest. 2009; 119

9. Rached MT, Kode A, Silva BC, Jung DY, Gray S, Ong H, Paik JH, DePinho RA, Kim JK, Karsenty G, Kousteni S. FoxO1 expression in osteoblasts regulates glucose homeostasis through regulation of osteocalcin in mice. J Clin Invest. Jan 4.2010 120:357–368. [PubMed: 20038793]

10. Corral DA, Amling M, Priemel M, Loyer E, Fuchs S, Ducy P, Baron R, Karsenty G. Dissociation between bone resorption and bone formation in osteopenic transgenic mice. Proc Natl Acad Sci U S A. Nov 10.1998 95:13835–13840. [PubMed: 9811887]

11. Pajvani UB, Trujillo ME, Combs TP, Iyengar P, Jelicks L, Roth KA, Kitsis RN, Scherer PE. Fat apoptosis through targeted activation of caspase 8: a new mouse model of inducible and reversible lipoatrophy. Nat Med. Jul.2005 11:797–803. [PubMed: 15965483]

12. Mallet VO, Mitchell C, Guidotti JE, Jaffray P, Fabre M, Spencer D, Arnoult D, Kahn A, Gilgenkrantz H. Conditional cell ablation by tight control of caspase-3 dimerization in transgenic mice. Nat Biotechnol. Dec.2002 20:1234–1239. [PubMed: 12434157]

13. Wencker D, Chandra M, Nguyen K, Miao W, Garantziotis S, Factor SM, Shirani J, Armstrong RC, Kitsis RN. A mechanistic role for cardiac myocyte apoptosis in heart failure. J Clin Invest. May. 2003 111:1497–1504. [PubMed: 12750399]

14. Heyman RA, Borrelli E, Lesley J, Anderson D, Richman DD, Baird SM, Hyman R, Evans RM. Thymidine kinase obliteration: creation of transgenic mice with controlled immune deficiency. Proc Natl Acad Sci U S A. Apr.1989 86:2698–2702. [PubMed: 2539597]

15. Salomon B, Lores P, Pioche C, Racz P, Jami J, Klatzmann D. Conditional ablation of dendritic cells in transgenic mice. J Immunol. Jan 15.1994 152:537–548. [PubMed: 8283035]

16. Soriano P. Generalized lacZ expression with the ROSA26 Cre reporter strain. Nat Genet. Jan.1999 21:70–71. [PubMed: 9916792]

17. Beck E, Ludwig G, Auerswald EA, Reiss B, Schaller H. Nucleotide sequence and exact localization of the neomycin phosphotransferase gene from transposon Tn5. Gene. Oct.1982 19:327–336. [PubMed: 6295884]

18. Adra CN, Boer PH, McBurney MW. Cloning and expression of the mouse pgk-1 gene and the nucleotide sequence of its promoter. Gene. 1987; 60:65–74. [PubMed: 3440520]

19. Yagi T, Ikawa Y, Yoshida K, Shigetani Y, Takeda N, Mabuchi I, Yamamoto T, Aizawa S. Homologous recombination at c-fyn locus of mouse embryonic stem cells with use of diphtheria toxin A-fragment gene in negative selection. Proc Natl Acad Sci U S A. Dec.1990 87:9918–9922. [PubMed: 2263643]

20. Valenzuela DM, Murphy AJ, Frendewey D, Gale NW, Economides AN, Auerbach W, Poueymirou WT, Adams NC, Rojas J, Yasenchak J, Chernomorsky R, Boucher M, Elsasser AL, Esau L, Zheng

J, Griffiths JA, Wang X, Su H, Xue Y, Dominguez MG, Noguera I, Torres R, Macdonald LE, Stewart AF, DeChiara TM, Yancopoulos GD. High-throughput engineering of the mouse genome coupled with high-resolution expression analysis. Nat Biotechnol. Jun.2003 21:652–659. [PubMed: 12730667]

21. Indra AK, Warot X, Brocard J, Bornert JM, Xiao JH, Chambon P, Metzger D. Temporally-controlled site-specific mutagenesis in the basal layer of the epidermis: comparison of the recombinase activity of the tamoxifen-inducible Cre-ER(T) and Cre-ER(T2) recombinases. Nucleic Acids Res. Nov 15.1999 27:4324–4327. [PubMed: 10536138]
22. Clemens TL, Tang H, Maeda S, Kesterson RA, DeMayo F, Pike JW, Gundberg CM. Analysis of osteocalcin expression in transgenic mice reveals a species difference in vitamin D regulation of mouse and human osteocalcin genes. J Bone Miner Res. Oct.1997 12:1570–1576. [PubMed: 9333117]
23. Bilic-Curcic I, Kronenberg M, Jiang X, Bellizzi J, Mina M, Marijanovic I, Gardiner EM, Rowe DW. Visualizing levels of osteoblast differentiation by a two-color promoter-GFP strategy: Type I collagen-GFPcyan and osteocalcin-GFPtpz. Genesis. Oct.2005 43:87–98. [PubMed: 16149065]
24. Zhao G, Monier-Faugere MC, Langub MC, Geng Z, Nakayama T, Pike JW, Chernausek SD, Rosen CJ, Donahue LR, Malluche HH, Fagin JA, Clemens TL. Targeted overexpression of insulin-like growth factor I to osteoblasts of transgenic mice: increased trabecular bone volume without increased osteoblast proliferation. Endocrinology. Jul.2000 141:2674–2682. [PubMed: 10875273]
25. Sims NA, White CP, Sunn KL, Thomas GP, Drummond ML, Morrison NA, Eisman JA, Gardiner EM. Human and murine osteocalcin gene expression: conserved tissue restricted expression and divergent responses to 1,25-dihydroxyvitamin D3 in vivo. Mol Endocrinol. Oct.1997 11:1695–1708. [PubMed: 9328351]
26. Kesterson RA, Stanley L, DeMayo F, Finegold M, Pike JW. The human osteocalcin promoter directs bone-specific vitamin D-regulatable gene expression in transgenic mice. Mol Endocrinol. 1993; 7:462–467. [PubMed: 8483481]
27. Ivanova A, Signore M, Caro N, Greene ND, Copp AJ, Martinez-Barbera JP. In vivo genetic ablation by Cre-mediated expression of diphtheria toxin fragment A. Genesis. Nov.2005 43:129–135. [PubMed: 16267821]
28. Brockschnieder D, Lappe-Siefke C, Goebbels S, Boesl MR, Nave KA, Riethmacher D. Cell depletion due to diphtheria toxin fragment A after Cre-mediated recombination. Mol Cell Biol. Sep.2004 24:7636–7642. [PubMed: 15314171]
29. Matsumura H, Hasuwa H, Inoue N, Ikawa M, Okabe M. Lineage-specific cell disruption in living mice by Cre-mediated expression of diphtheria toxin A chain. Biochem Biophys Res Commun. Aug 20.2004 321:275–279. [PubMed: 15358172]
30. Ferron M, Hinoi E, Karsenty G, Ducy P. Osteocalcin differentially regulates beta cell and adipocyte gene expression and affects the development of metabolic diseases in wild-type mice. Proc Natl Acad Sci U S A. Apr 1.2008 105:5266–5270. [PubMed: 18362359]
31. Yamauchi T, Kamon J, Waki H, Terauchi Y, Kubota N, Hara K, Mori Y, Ide T, Murakami K, Tsuboyama-Kasaoka N, Ezaki O, Akanuma Y, Gavrilova O, Vinson C, Reitman ML, Kagechika H, Shudo K, Yoda M, Nakano Y, Tobe K, Nagai R, Kimura S, Tomita M, Froguel P, Kadowaki T. The fat-derived hormone adiponectin reverses insulin resistance associated with both lipoatrophy and obesity. Nat Med. Aug.2001 7:941–946. [PubMed: 11479627]
32. Steppan CM, Bailey ST, Bhat S, Brown EJ, Banerjee RR, Wright CM, Patel HR, Ahima RS, Lazar MA. The hormone resistin links obesity to diabetes. Nature. Jan 18.2001 409:307–312. [PubMed: 11201732]
33. Friedman JM, Halaas JL. Leptin and the regulation of body weight in mammals. Nature. Oct 22.1998 395:763–770. [PubMed: 9796811]
34. Wolfrum C, Asilmaz E, Luca E, Friedman JM, Stoffel M. Foxa2 regulates lipid metabolism and ketogenesis in the liver during fasting and in diabetes. Nature. Dec 23.2004 432:1027–1032. [PubMed: 15616563]
35. Puigserver P, Rhee J, Donovan J, Walkey CJ, Yoon JC, Oriente F, Kitamura Y, Altomonte J, Dong H, Accili D, Spiegelman BM. Insulin-regulated hepatic gluconeogenesis through FOXO1-PGC-1alpha interaction. Nature. May 29.2003 423:550–555. [PubMed: 12754525]

36. Oury, F.; Sumara, G.; Sumara, O.; Ferron, M.; Chang, H.; Smith, CE.; Hermo, L.; Suarez, S.; Roth, BL.; Ducy, P.; Karsenty, G. Endocrine Regulation of Male Fertility by the Skeleton. 2011.

37. Bianco P, Riminucci M, Gronthos S, Robey PG. Bone marrow stromal stem cells: nature, biology, and potential applications. Stem Cells. 2001; 19:180–192. [PubMed: 11359943]

38. Moerman EJ, Teng K, Lipschitz DA, Lecka-Czernik B. Aging activates adipogenic and suppresses osteogenic programs in mesenchymal marrow stroma/stem cells: the role of PPAR-gamma2 transcription factor and TGF-beta/BMP signaling pathways. Aging Cell. Dec.2004 3:379–389. [PubMed: 15569355]

39. Shockley KR, Lazarenko OP, Czernik PJ, Rosen CJ, Churchill GA, Lecka-Czernik B. PPARgamma2 nuclear receptor controls multiple regulatory pathways of osteoblast differentiation from marrow mesenchymal stem cells. J Cell Biochem. Feb 1.2009 106:232–246. [PubMed: 19115254]

40. Kang S, Bennett CN, Gerin I, Rapp LA, Hankenson KD, MacDougald OA. Wnt signaling stimulates osteoblastogenesis of mesenchymal precursors by suppressing CCAAT/enhancer-binding protein alpha and peroxisome proliferator-activated receptor gamma. J Biol Chem. May 11.2007 282:14515–14524. [PubMed: 17351296]

41. Kawaguchi H, Akune T, Yamaguchi M, Ohba S, Ogata N, Chung UI, Kubota N, Terauchi Y, Kadowaki T, Nakamura K. Distinct effects of PPARgamma insufficiency on bone marrow cells, osteoblasts, and osteoclastic cells. J Bone Miner Metab. 2005; 23:275–279. [PubMed: 15981022]

42. Lazarenko OP, Rzonca SO, Hogue WR, Swain FL, Suva LJ, Lecka-Czernik B. Rosiglitazone induces decreases in bone mass and strength that are reminiscent of aged bone. Endocrinology. Jun.2007 148:2669–2680. [PubMed: 17332064]

43. Hesslein DG, Fretz JA, Xi Y, Nelson T, Zhou S, Lorenzo JA, Schatz DG, Horowitz MC. Ebf1-dependent control of the osteoblast and adipocyte lineages. Bone. Apr.2009 44:537–546. [PubMed: 19130908]

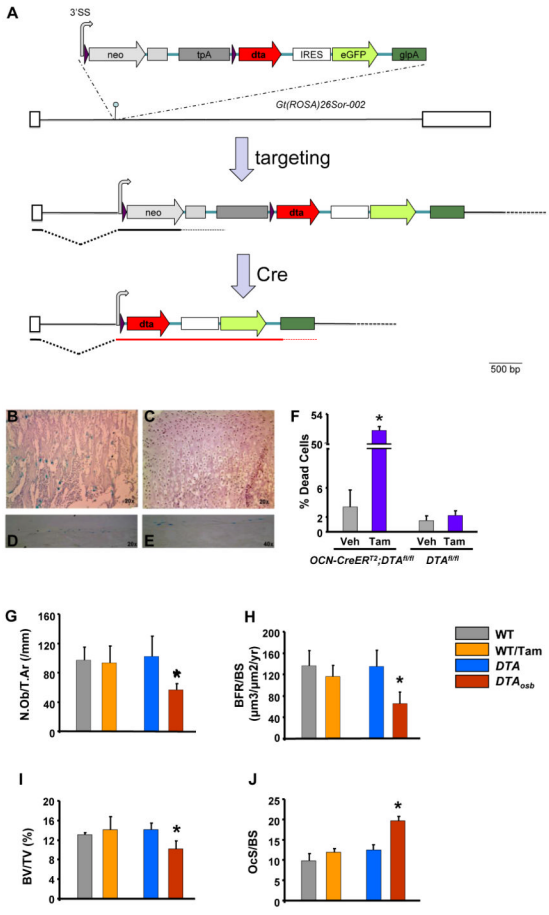

Figure 1. Inducible, partial osteoblast ablation in *DTA$_{osb}$* mice

(A) The 3′SS-LoxP-EM7-neo-pgkpolyA-tpA-LoxP-dta-ires-eGFP-ßglpA transgene was targeted at the *Gt(ROSA)26Sor* locus into the XbaI site (hairpin). Only the 002 isoform of *Gt(ROSA)26Sor* is shown, adapted from Ensembl (release 60 - Nov 2010). Exons are shown as white boxes, whereas native intronic sequences are depicted by a black line. *LoxP* sites (purple arrows) flank the *EM7-neo-pgkpolyA-tpA* part of the transgene, enabling its deletion by Cre and concomitant activation of *DTA* expression. The shared 3′ splice site (3′SS) is shown as a gray curved arrow (hence also marking the direction of transcription. The *pgkpolyA* immediately following neo is shown as a gray box. The triple *polyA (tpA)* derived from SV40 is shown as a dark gray box. The intact locus expresses only *neo*. After exposure to Cre, the floxed region is deleted and expression of *DTA* is activated. Neo, neomycin phoshotransferase ORF; tpA, triple polyA; DTA, diphtheria toxin A; IRES, internal ribosome entry site; eGPF, enhanced Green Fluorescent Protein; glpA, rabbit beta globin polyA region. **(B-J)** Eight week-old mice were injected intraperitoneally with vehicle or 0.07mg/g of tamoxifen daily for 10 days. Three days later animals were euthanized and femurs were harvested. Cre expression was examined by assessing β-gal activity in the femurs. For this purpose, whole mount femurs were stained using X-gal, a chromogenic substrate for β-gal. Tissues expressing β-gal are stained with a blue color. Sections shown in the top 2 panels (B and C) were counterstained with eosin whereas sections in panels C and D were not counterstained. All sections were mounted in DPX. Images were acquired with a Nikon 80i Eclipse Microscope using a Retiga digital camera. **(B)** In the primary spongiosa of femurs obtained from *ROSA26-lacZ* and *OCN-CreER^{T2}* double mutant mice osteoblastic cells expressing β-gal appear blue. **(C)** There was no staining observed in vehicle-treated

double mutant animals. Panels **(D)** and **(E)** show two different magnifications of the femoral midshaft in *ROSA26-lacZ* and *OCN-CreER^{T2}* double mutant mice treated with tamoxifen. **(F)** Calvaria cells were isolated from *DTA$^{fl/fl}$*;*OCN-CreER^{T2}* (*DTA* mice) or from *DTA$^{fl/fl}$* (WT mice) control animals. Cells were differentiated in the presence of 50 μM ascorbic acid and β-glycerophosphate for 10 days. Tamoxifen (10^{-8} M) was added to cultures for 6 hours. Apoptosis was assessed by trypan blue exclusion. Each bar represents individual readings from cells isolated from 6 double mutant and 4 control animals. *p<0.05 vs. vehicle. **(G-J)** N.Ob/T.Ar, number of osteoblasts per trabecular area; BFR, bone formation rate; BV/TV, bone volume over trabecular volume and OcS/BS, osteoclast surface over bone surface in vertebrae of 2 month-old WT, *DTA* and *DTA$_{osb}$* mice (n=8 mice/group). Bars indicate means ± s.e.m *p<0.05 vs WT and *DTA* and WT/tamoxifen.

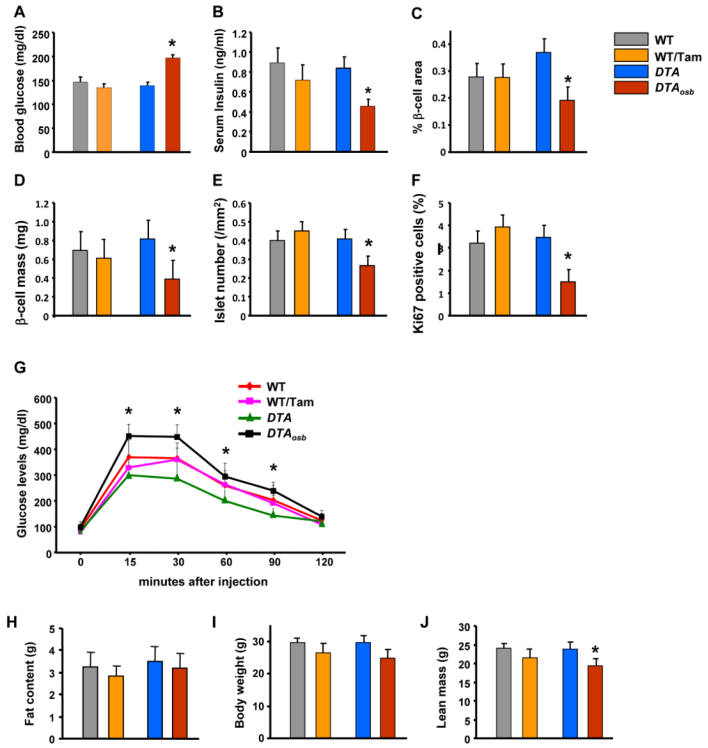

Figure 2. Osteoblast ablation compromises glucoses homeostasis

(A) Blood glucose and **(B)** serum insulin levels in WT and *DTA*$_{osb}$ mice at random feeding. **(C-E)** H&E and insulin staining was used to calculate islet numbers and β-cell area and mass. **(F)** Ki67 immunostaining showed decreased β-cell proliferation in the pancreas of *DTA*$_{osb}$ mice. **(G)** Glucose tolerance test (GTT) in WT and *DTA*$_{osb}$ mice. **(H)** total fat content, **(I)** Body weight, and **(J)** lean body mass in *DTA*$_{osb}$ mice. In (J)-(S) n=5 mice/group. In all panels except D and J bars indicate means ± s.e.m *p<0.05 vs WT and *DTA* and WT/tamoxifen. In D and J *p<0.05 vs WT and DTA. All mice were 2 months of age.

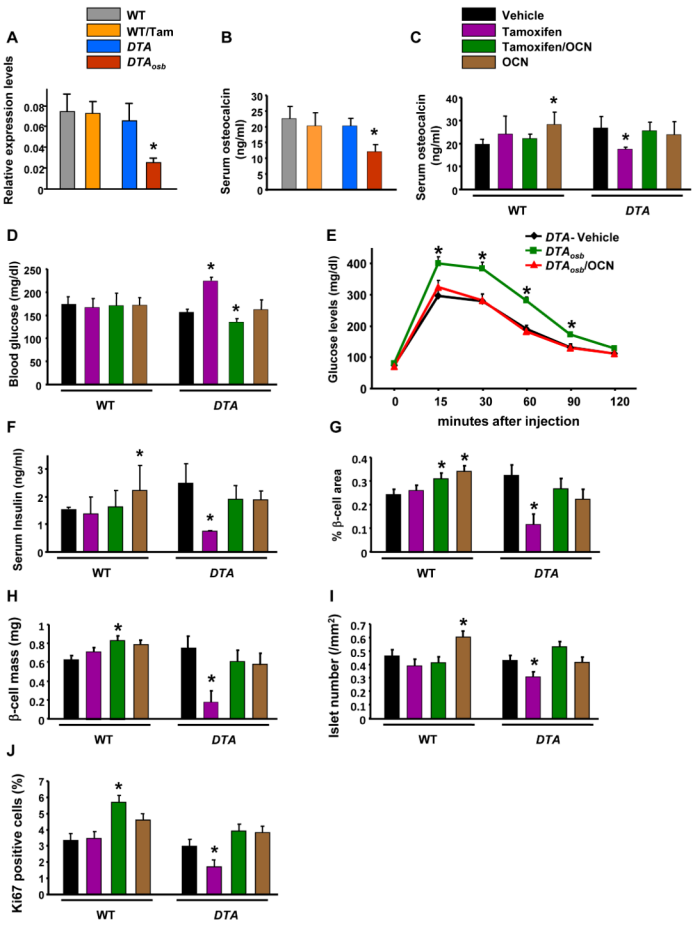

Figure 3. Compromised glucose metabolism and insulin secretion are rescued by Osteocalcin treatment in mice lacking osteoblasts

(A) Real time PCR analysis of osteocalcin expression in bone and **(B)** and **(C)** serum osteocalcin levels in DTA_{osb} and osteocalcin-treated DTA_{osb} mice. **(D)** Blood glucose, and **(E)** glucose tolerance test in DTA_{osb} mice. **(F)** Serum insulin levels, **(G)** Islet numbers, **(H)** β-cell area, **(I)** β-cell mass and **(J)** β-cell proliferation in osteocalcin-treated DTA_{osb} (*DTA*/Tamoxifen/OCN) mice. In all experiments n=5-8 mice/group. In all panels bars indicate means ± s.e.m *p<0.05 vs WT/vehicle and WT/Tamoxifen and *DTA*/vehicle. All mice were 2 months of age.

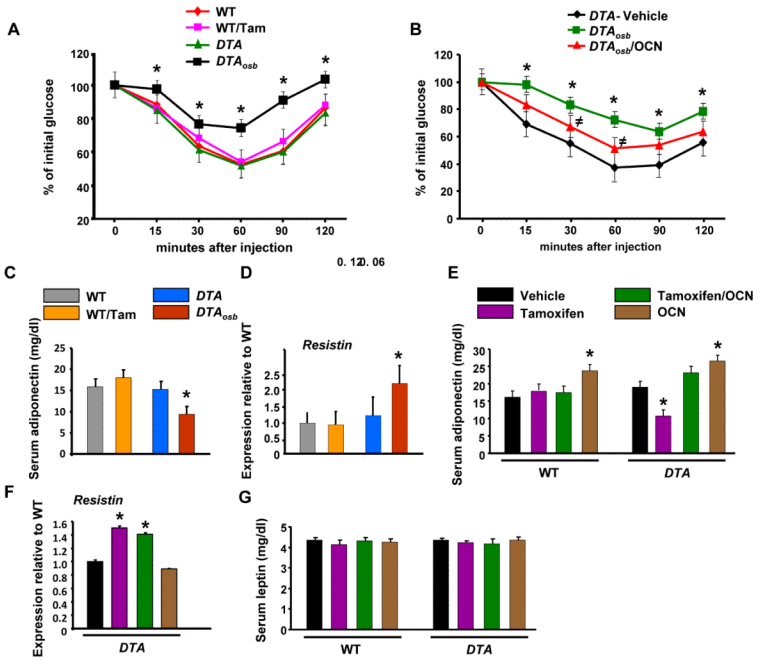

Figure 4. Insulin insensitivity in osteoblast-depleted mice is partially reversed by Osteocalcin

(A) and **(B)** Insulin tolerance tests (ITT) in WT and DTA_{osb} mice. *p<0.05 vs WT/vehicle and $^{\neq}p$<0.05 vs DTA_{osb} **(C)** and **(E)** Serum adiponectin levels, **(D)** and **(F)** real-time PCR analysis of *resistin* expression in white fat and **(G)** serum leptin levels in WT and osteocalcin-treated DTA_{osb} (*DTA*/Tamoxifen/OCN) mice. In (A)-(G) n=5-8 mice/group. In all panels except (B) *p<0.05 vs WT/vehicle and WT/Tamoxifen and *DTA*/vehicle, In all panels bars indicate means ± s.e.m *p<0.05. All mice were 2 months of age.

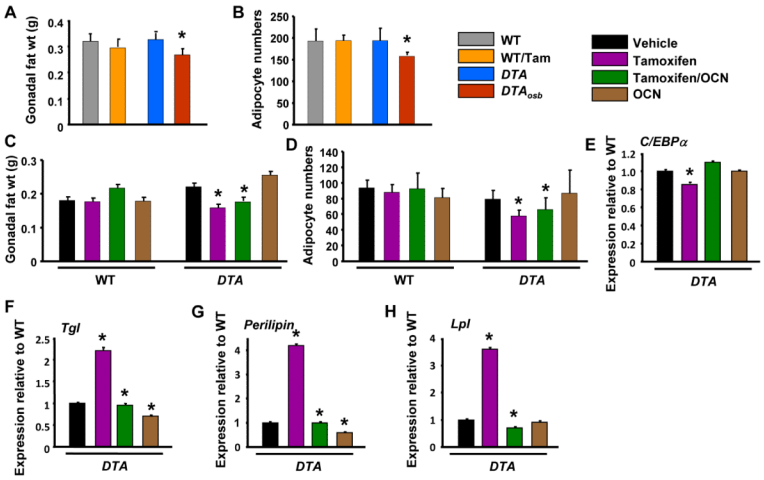

Figure 5. Increased fat metabolism in osteoblast-depleted mice is not affected by Osteocalcin

(A) Gonadal fat pad weight and **(B)** adipocyte numbers in WT and DTA_{osb} mice, n=7 mice/group. **(C)** Gonadal fat pad weight and **(D)** adipocyte numbers in osteocalcin-treated WT and DTA_{osb} (*DTA*/Tamoxifen/OCN) mice, n=7 mice/group. **(E-H)** Real-time PCR analysis of insulin target genes in white fat of vehicle, tamoxifen or osteocalcin-treated *DTA* mice, n=7 mice/group. In all panels bars indicate means ± s.e.m *p<0.05 vs WT/vehicle and WT/Tamoxifen and *DTA*/vehicle. In A p<0.05 vs WT/vehicle and *DTA*/vehicle. All mice were 2 months of age.

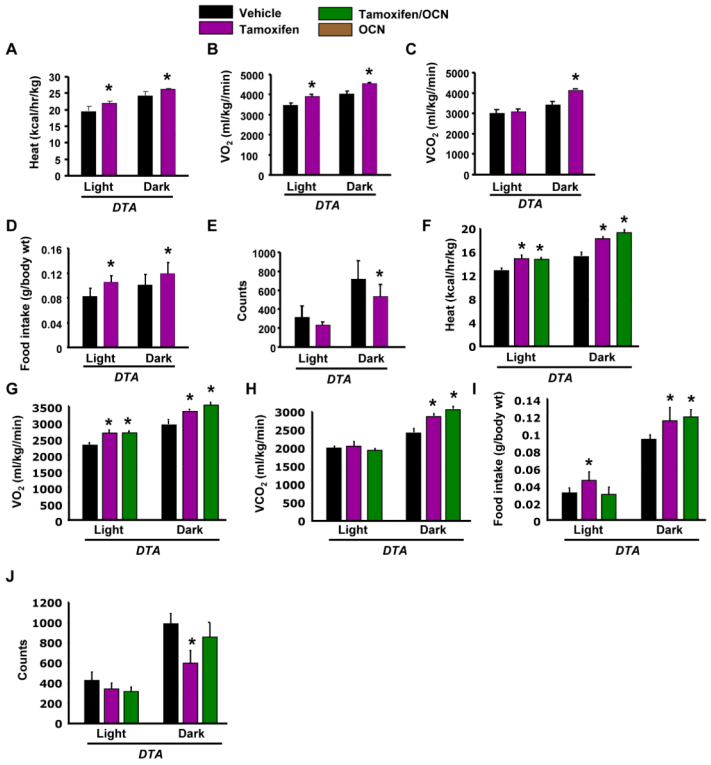

Figure 6. Increased energy expenditure in osteoblast-depleted mice is not affected by Osteocalcin

(A-E) Heat production, oxygen consumption, CO_2 expenditure, food intake and total activity (counts) by indirect calorimetric analysis in WT and DTA_{osb} mice, n=4 mice/group. **(F-J)** Heat production, oxygen consumption, CO_2 expenditure, food intake and total activity (counts) by indirect calorimetric analysis in vehicle, tamoxifen or osteocalcin-treated *DTA* mice, n=4 mice/group. In all panels bars indicate means ± s.e.m *p<0.05 vs WT/vehicle and WT/Tamoxifen and *DTA*/vehicle. All mice were 2 months of age.

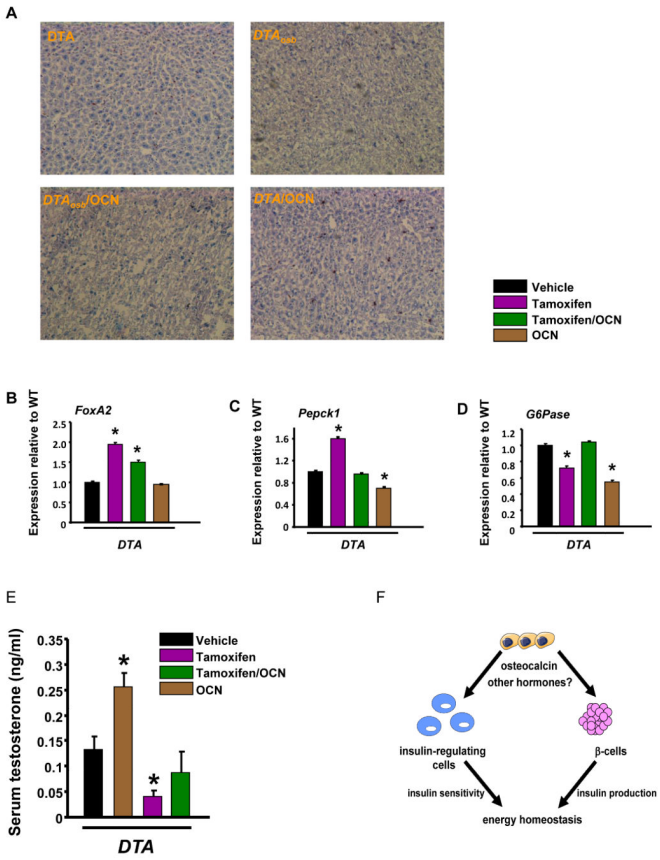

Figure 7. Insulin signaling in the liver of osteoblast-depleted mice is not affected by Osteocalcin

(A) Oil red O staining in liver sections of WT and osteocalcin-treated DTA_{osb} mice. Scale bars are 100 μm. Real-time PCR analysis of **(B)** *FoxA2* expression in the liver of WT and osteocalcin-treated DTA_{osb} (*DTA*/Tamoxifen/OCN) mice. **(C)** *Pepck1* and **(D)** *G6pase* in osteocalcin-treated DTA_{osb} (*DTA*/Tamoxifen/OCN) mice. In (A)-(L) n=5-8 mice/group. **(E)** Serum testosterone levels in WT and osteocalcin-treated DTA_{osb} (*DTA*/Tamoxifen/OCN) mice. In all panels except (A) *p<0.05 vs WT/vehicle and WT/Tamoxifen and *DTA*/vehicle. All mice were 2 months of age. (F). Osteoblasts act through osteocalcin and perhaps other hormones to affect both the function of β-cells as well as that of other insulin responsive cells in insulin target organs that are sources of glucose production or regulate insulin sensitivity. The total outcome of these interactions is to maintain energy homeostasis.

Table 1

Comparison of the metabolic changes induced by osteoblast or osteocalcin deficiency and osteocalcin rescue (Y: yes; N: no)

Metabolic parameter	Osteoblast deficiency	Osteocalcin rescue	Osteocalcin deficiency
Blood glucose	↑	Y	↑
Glucose tolerance	↓	Y	↓
Blood insulin	↓	Y	↓
β-cell proliferation	↓	Y	↓
Insulin sensitivity	↓	Partial	↓
Adiponectin	↓	Y	↓
Resistin	↑	N	—
Leptin	—	N	—
Body weight	—	N	—
Gonadal Fat	↓	N	↑
Adipocyte number	↓	N	↑
Energy expenditure	↑	N	↓
Food intake	↑	N	—
Movement	↓	N	—
Ketogenesis/lipogenesis	↓	N	↑